

Processes $e^-e^+ \rightarrow \gamma\gamma, Z\gamma, ZZ$ in the standard model and the minimal supersymmetric standard model

G. J. Gounaris

Department of Theoretical Physics, Aristotle University of Thessaloniki, Gr-54124, Thessaloniki, Greece

J. Layssac and F. M. Renard

Physique Mathématique et Théorique, UMR 5825, Université Montpellier II, F-34095 Montpellier Cedex 5, France

(Received 23 July 2002; revised manuscript received 5 November 2002; published 31 January 2003)

We present the results of a complete analysis of the one-loop electroweak corrections to $e^-e^+ \rightarrow \gamma\gamma, Z\gamma, ZZ$ in the standard model (SM) and the minimal supersymmetric standard model (MSSM). A special emphasis is put on the high energy behavior of the various helicity amplitudes and the way the logarithmic structure is generated. The large magnitude of these effects, which induce striking differences between the SM and MSSM cases at high energies, offers the possibility of making global tests which could check the consistency of these models, and even decide whether any additional new physics is required.

DOI: 10.1103/PhysRevD.67.013012

PACS number(s): 12.15.Lk, 12.60.Jv, 14.70.-e

I. INTRODUCTION

Several projects of high energy and high luminosity e^-e^+ colliders [Linear Collider (LC), CERN Linear Collider (CLIC)] are under consideration [1,2], possibly with a photon-photon option [3]. They should allow us not only to produce new particles but also to make very precise tests of the fundamental interactions.

It is by now well known that the electroweak radiative corrections to several standard processes strongly increase with energy. This arises due to the presence, already at the one-loop level, of large double (DL) and single (SL) logarithm terms behaving like $(\alpha/\pi)\ln^2 s$, $(\alpha/\pi)\ln s$, [4–6]. In the TeV range such terms reach the several tens of percent level. They are no more “small corrections” of order α/π as in the CERN e^+e^- collider LEP SLAC Linear Collider (SLC) energy range; they are essential parts of the dynamics.

A very important property of these large DL and SL logarithmic terms is that their coefficients reflect the gauge and Higgs structure of the basic interactions. Thus they offer a striking signature for studying the underlying dynamics and differentiate between the standard model (SM) and the minimal supersymmetric standard model (MSSM) [7,8]. Compared with the high level of the experimental accuracy (few per mille) that is expected for future colliders, this should allow deep tests of the basic electroweak interactions.

This has been illustrated recently by showing the relevance of the SL and DL terms at high energy colliders in the case of light and heavy fermion pair production in e^+e^- [6,9] and $\gamma\gamma$ [10] collisions, and also for sfermion pair production [11]. Corrections including higher order contributions have also been computed [11,12].

Alternatively, these large logarithmic effects may also appear as large background contributions to possible new physics (NP) signals. It will therefore be essential to have full control on them, which necessitates a precise analysis of the various virtual contributions induced from each dynamical sector. This will be particularly important in case a departure is observed and hints for its origin are examined.

The aim of this paper is to discuss these aspects in the case of neutral gauge boson pair production in $e^+e^- \rightarrow \gamma\gamma, Z\gamma, ZZ$. One-loop effects in the SM have already been computed some time ago [13]. The additional step here is to analyze in detail the high energy behavior and consider also the complete set of MSSM contributions. We examine how the asymptotic [double log (DL) and single log (SL)] contributions are generated using the complete expressions in each of the gauge and Higgs sectors, in SM and MSSM. This should also be useful for discussing possible modifications due to NP, and proposing strategies for comparing with experimental results.

Incidentally, the neutral gauge boson production processes $e^+e^- \rightarrow Z\gamma, ZZ$ received recently considerable theoretical [14–16] and experimental [17] interest motivated by the search for anomalous neutral gauge boson self-couplings (NAGC). At the tree level in the SM and MSSM no couplings exist among three neutral gauge bosons. Such couplings only appear at one loop, through fermion triangles involving leptons and quarks in the SM, and also charginos and neutralinos in MSSM [15]. These contributions are of course part of the complete one-loop corrections mentioned above. The interest in them though is that additional such contributions may appear, induced from NP forms containing, e.g., heavier fermions, nonperturbative structures, or even direct neutral boson couplings. To experimentally study such couplings, it is essential to have full control of the “normal” SM or MSSM corrections; we will devote a special discussion to this point.

Finally, we consider the role of longitudinal Z production. At high energy the Z_L production in the SM and MSSM is strongly depressed; but the depression is stronger at the Born level than after radiative corrections are included. As a result, the Born contribution to, e.g., $Z_L Z_L$ production above 1 TeV, is negligible compared to the one-loop one. Such a channel may be a suitable place to search for forms of anomalous NP contribution generated by, e.g., a strongly interacting Higgs sector.

The paper is organized as follows. In Sec. II we describe

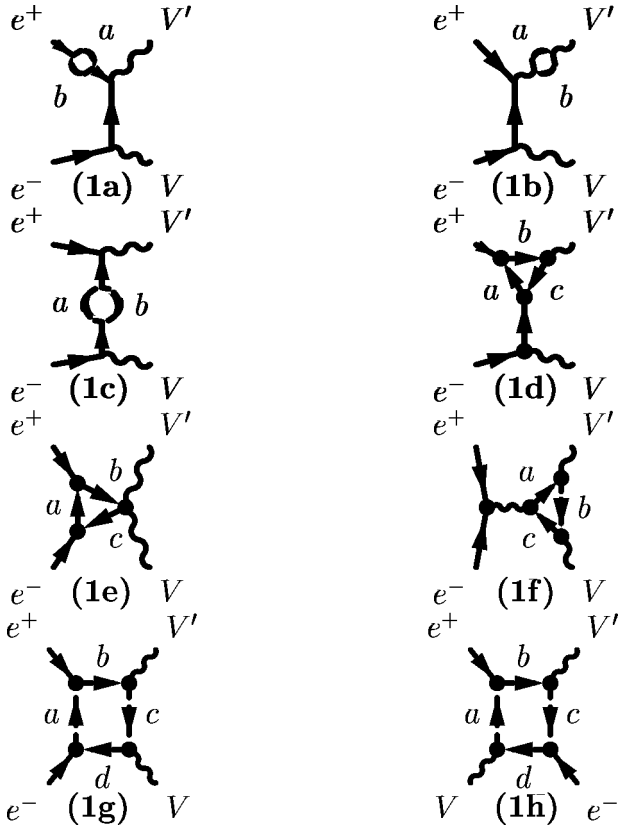


FIG. 1. Diagrams at one loop.

the method used for the computation of the one-loop contributions and we give the explicit expressions of the asymptotic amplitudes. The numerical results are presented in Sec. III and we conclude in Sec. IV. In the Appendix we define our notations and give the expression of the Born terms.

II. THE ONE-LOOP CONTRIBUTIONS

In the present work, the complete one-loop effects in $e^-e^+ \rightarrow \gamma\gamma, Z\gamma, ZZ$ have been computed, using the on-shell renormalization formalism [18]. The relevant diagrams are depicted in Fig. 1. The results are expressed in terms of invariant amplitudes N_j defined in the Appendix. We refrain from giving the explicit expressions of the invariant amplitudes in this short paper, since they can be found in the archives [19]. The structure of these amplitudes is

$$N_j(s, t, u) = N_j^{\text{ren+Born}} + N_j^{\text{Tri}} + N_j^{\text{Box}}, \quad (1)$$

where $N_j^{\text{ren+Born}}$ represents the Born amplitudes modified by renormalization counterterms and the gauge and electron self-energy functions. The other two terms in Eq. (1) describe the triangular and box diagram contributions. The SM contribution is then fully determined by diagrams involving only standard particle exchanges; while in the MSSM case additional diagrams arise involving SUSY contributions to self-energies and the triangle and box diagrams containing chargino, neutralino, slepton, squark, and charged and neu-

tral Higgs exchanges. The couplings and masses are taken from [20], and the neutralino mixing formalism of [21] is used.

In the illustrations we use the specific benchmark MSSM models corresponding to typical cases with either low or high masses for the inos or the sfermions [22,23]. These models are constructed in the context of the constrained MSSM supergravity (SUGRA) framework, with universal soft supersymmetry-breaking masses, assuming R -parity conservation. They have been selected to be consistent with all present particle physics and cosmological constraints, and provide a rough indication of all available possibilities in the SUGRA framework [22].

The one-loop amplitudes are quite involved. They become simple and intuitive though at very high energies, whenever $(s, |t|, |u|)$ are much larger than all masses of the particles exchanged in the various diagrams. Under such conditions, the dominant radiative corrections are described by single (SL) and double-log (DL) corrections affecting only those N_j which receive nonvanishing Born-level contributions [these Born amplitudes are given in Eqs. (A10)–(A14)].

Thus, to the leading-log approximation, the radiatively corrected invariant amplitudes are given by

$$N_j \approx N_j^{\text{Born},L} [1 + c_L] + N_j^{\text{Born},R} [1 + c_R] + d_{j,L}^{(W)}, \quad (2)$$

where only the invariant amplitudes N_j for which the Born contribution is nonvanishing, appear. The $c_{L,R}$ coefficients are process, model, and j -independent. In the SM case, they are given by

$$c_L = \frac{\alpha(1 + 2c_W^2)}{16\pi s_W^2 c_W^2} \left[3 \ln \frac{s}{m_W^2} - \ln^2 \frac{s}{m_W^2} \right] - \frac{\alpha a^{(W)}}{8\pi s_W^2} \ln^2 \frac{s}{m_W^2}, \quad (3)$$

$$c_R = \frac{\alpha}{4\pi c_W^2} \left[3 \ln \frac{s}{m_W^2} - \ln^2 \frac{s}{m_W^2} \right], \quad (4)$$

while in the MSSM case by

$$c_L = \frac{\alpha(1 + 2c_W^2)}{16\pi s_W^2 c_W^2} \left[2 \ln \frac{s}{m_W^2} - \ln^2 \frac{s}{m_W^2} \right] - \frac{\alpha a^{(W)}}{8\pi s_W^2} \ln^2 \frac{s}{m_W^2}, \quad (5)$$

$$c_R = \frac{\alpha}{4\pi c_W^2} \left[2 \ln \frac{s}{m_W^2} - \ln^2 \frac{s}{m_W^2} \right], \quad (6)$$

where in the right-hand part of Eqs. (3) and (5)

$$a^{(W)} = -2, \quad \frac{3 - 4s_W^2}{1 - 2s_W^2}, \quad \frac{4c_W^2}{1 - 2s_W^2}, \quad (7)$$

should be used for $\gamma\gamma$, γZ , and ZZ , respectively.

As seen from Eq. (2), (c_L, c_R) provide angular-independent universal corrections to the Born amplitudes. In addition to them though, the additive W -box contributions $d_{j,L}^{(W)}$ appear in Eq. (2), which are discussed below.

The $c_{L,R}$ correction in Eq. (2) is (a least partly) induced by vertex diagrams involving photon, Z , W , and MSSM partner exchanges. In particular, the first terms for c_L and the complete c_R terms [compare Eqs. (3)–(6)], which have the structure

$$\left[3 \ln\left(\frac{s}{m_W^2}\right) - \ln^2\left(\frac{s}{m_W^2}\right) \right] \quad \text{in SM,}$$

$$\left[2 \ln\left(\frac{s}{m_W^2}\right) - \ln^2\left(\frac{s}{m_W^2}\right) \right] \quad \text{in MSSM,} \quad (8)$$

are generated by diagrams involving an electron line and satisfy the same rules as those established in [8,10] for fermion and scalar pair production in e^-e^+ annihilation. In agreement with [8,10], we find that their coefficients are independent of the SM or MSSM scales, depending only on the e_L, e_R weak isospin I_e and hypercharge $Y_e \equiv 2(Q_e - I_e^{(3)})$, through

$$\frac{\alpha}{4\pi} \left[\frac{I_e(I_e+1)}{s_W^2} + \frac{Y_e^2}{4c_W^2} \right]. \quad (9)$$

Thus (as far as the electron-line terms are concerned) at energies much larger than the masses of all standard and supersymmetric particles, the only difference between SM and MSSM dynamics is concentrated in changing the SL coefficient from 3 to 2, obviously because of the different number of degrees of freedom in the two models. On the contrary, the double-log term DL is the same in both the SM and MSSM dynamics [8,10].

The last $a^{(W)}$ terms in Eqs. (3), (5) come from subgraphs involving the final gauge bosons and only contain DL terms. As in the electron-line case, the coefficients of these DL terms are insensitive to the differences between the SM and MSSM dynamics; they are given in Eq. (7).

The $d_{j,L}^{(W)}$ term in Eq. (2) is a specific purely standard W -box contribution, whose coefficient is fixed by the γWW and ZWW couplings. It is angular dependent and of course, insensitive to supersymmetric particle exchanges. It is given by

$$d_{j,L}^{(W)} = \frac{\alpha^2 b^{(W)}}{s_W^2} P_L \left\{ \eta_t^j \left[2 \ln \frac{s}{m_W^2} \ln \frac{1 - \cos \theta}{2} + \ln^2 \frac{1 - \cos \theta}{2} \right] \right. \\ \left. + \eta_u^j \left[2 \ln \frac{s}{m_W^2} \ln \frac{1 + \cos \theta}{2} + \ln^2 \frac{1 + \cos \theta}{2} \right] \right\}, \quad (10)$$

where again the index j runs over the N_j amplitudes that receive nonvanishing Born contribution. For $\gamma\gamma$ production, the parameters to be used in Eq. (10) are

$$b^{(W)} = 1, \quad \eta_t^{1,2} = \frac{1}{t},$$

$$\eta_t^4 = \frac{1}{t} + \frac{2}{s}, \quad \eta_u^{1,2} = \frac{1}{u}, \quad \eta_u^4 = -\frac{1}{u} - \frac{2}{s}, \quad (11)$$

while, for γZ ,

$$b^{(W)} = 1/4s_W c_W,$$

$$\eta_t^{1,2} = -\frac{s}{2} \eta_t^6 = \frac{3 - 4s_W^2}{t} - \frac{1}{u},$$

$$\eta_u^{1,2} = -\frac{s}{2} \eta_u^6 = \frac{3 - 4s_W^2}{u} - \frac{1}{t},$$

$$\eta_t^4 = \frac{3 - 4s_W^2}{t} + \frac{1}{u} + \frac{8c_W^2}{s}, \quad \eta_u^4 = -\frac{3 - 4s_W^2}{u} - \frac{1}{t} - \frac{8c_W^2}{s}, \quad (12)$$

$$\eta_t^5 = \frac{1}{u} + \frac{4c_W^2}{s}, \quad \eta_u^5 = -\frac{3 - 4s_W^2}{u} - \frac{4c_W^2}{s},$$

and, for ZZ ,

$$b^{(W)} = 1/2s_W^2,$$

$$\eta_t^{1,2} = \frac{1 - 2s_W^2}{t} - \frac{1}{u}, \quad \eta_u^{1,2} = \frac{1 - 2s_W^2}{u} - \frac{1}{t},$$

$$\eta_t^4 = \frac{1 - 2s_W^2}{t} + \frac{1}{u} + \frac{4c_W^2}{s}, \quad \eta_u^4 = -\frac{1 - 2s_W^2}{u} - \frac{1}{t} - \frac{4c_W^2}{s},$$

$$\eta_t^5 = \frac{1}{u} + \frac{2c_W^2}{s}, \quad \eta_u^5 = -\frac{1 - 2s_W^2}{u} - \frac{2c_W^2}{s}, \quad (13)$$

$$\eta_t^6 = -\eta_t^8 = -\frac{2}{s} \left[\frac{1 - 2s_W^2}{t} - \frac{1}{u} \right],$$

$$\eta_u^6 = -\eta_u^8 = -\frac{2}{s} \left[\frac{1 - 2s_W^2}{u} - \frac{1}{t} \right],$$

$$\eta_t^7 = \frac{2s_W^2 - 1}{t} - \frac{2c_W^2}{s}, \quad \eta_u^7 = \frac{1}{t} + \frac{2c_W^2}{s}.$$

When the helicity amplitudes generated by the N_j ones are computed, it is found that the above structure of mainly multiplicative corrections to the Born contributions is only preserved for the TT amplitudes, where both final gauge bosons are transverse. It is only in this case that the one-loop asymptotic amplitudes are given by the Born ones, multiplied by the various leading-log coefficients. Such a factorization form does not work for the TL, LT, and LL, helicity amplitudes, which are mass suppressed; thereby forcing the difference between the high energy behavior of the one-loop helicity amplitude, and its Born contribution, to be not simply logarithmic, but to also have a power-law part.

As an example we recall that due to ‘‘gauge cancellations,’’ the Born $e^-e^+ \rightarrow ZZ$ TT amplitudes behave like a constant at asymptotic energies, the Born TL and LT ones vanish like m_Z/\sqrt{s} , and the Born LL amplitudes diminish like m_Z^2/s . This latter property can be explicitly seen in

$$F_{\lambda 00}^{\text{Born}} \simeq -(2\lambda) \frac{16m_Z^2 \cos \theta}{s \sin \theta} \left\{ \frac{(2s_W^2 - 1)^2}{4s_W^2 c_W^2} P_L + \frac{s_W^2}{c_W^2} P_R \right\}. \quad (14)$$

When the one-loop effects are included, the TL and LT amplitudes receive, apart from the logarithmic factors, additional mass dependent terms of the type M/\sqrt{s} , where M is some mass involved in the one-loop diagrams. For $Z_L Z_L$ amplitudes, these one-loop modifications lead to a strikingly different high energy structure, where the rapidly vanishing $\sim m_Z^2/s$ Born behavior is replaced by a logarithmically increasing one involving $\ln^2|t|/M^2$ and $\ln^2|u|/M^2$ terms. This structure is induced by Higgs sector box diagrams, whose asymptotic contribution dominates the tree-level one.

The simplest way to obtain it is by using the equivalence theorem and considering the processes $e^+e^- \rightarrow G^0 G^0$ (G^0 being the Goldstone state supplying the longitudinal Z_L component). Since in the $m_e=0$ limit this later process has no Born term, its only possible contribution comes from boxes with internal ($eZHZ$) and (νWGW) lines; where H stands for the standard Higgs boson in SM, while in MSSM it represents a suitable mixture of the CP -even H^0 and the h^0 states. The resulting asymptotic helicity amplitudes are then

$$\begin{aligned} F_{\lambda 00} &\simeq (2\lambda) \frac{\alpha^2 \sin \theta}{4} \left\{ \left[\ln^2 \frac{|t|}{m_W^2} - \ln^2 \frac{|u|}{m_W^2} \right] \right. \\ &\quad \times \left. \left\{ \left(\frac{1}{s_W^4} + \frac{(2s_W^2 - 1)^2}{2s_W^4 c_W^4} \right) P_L + \left(\frac{2}{c_W^4} \right) P_R \right\} \right\} \\ &\simeq (2\lambda) \frac{\alpha^2 \sin \theta}{2} \ln \left(\frac{s}{m_W^2} \right) \ln \left(\frac{1 - \cos \theta}{1 + \cos \theta} \right) \\ &\quad \times \left\{ \left(\frac{1}{s_W^4} + \frac{(2s_W^2 - 1)^2}{2s_W^4 c_W^4} \right) P_L + \left(\frac{2}{c_W^4} \right) P_R \right\}, \quad (15) \end{aligned}$$

in both SM and MSSM. Thus, at sufficiently high energy, the order α^2 contribution of Eq. (15) becomes larger than the (suppressed) Born LL contribution of Eq. (14). The cross-over of these two terms is around 1 TeV.

Contrary to the TT case induced by Eq. (2), asymptotically there is no difference between the SM and the MSSM predictions for longitudinal $Z_L Z_L$ production. This is due to the fact that the H^0 contribution is proportional to $\cos^2(\beta - \alpha)$ and the h^0 one proportional to $\sin^2(\beta - \alpha)$, producing a result identical to the SM one.

The NAGC effects

As mentioned in the Introduction, the full one-loop results for $e^-e^+ \rightarrow Z\gamma, ZZ$ in SM or MSSM may be viewed as an irreducible background in the search of possible anomalous neutral gauge boson couplings. The general form of such couplings has been written in [14]. Here, we restrict the analysis to the on-shell couplings $h_3^{\gamma,Z}$ and $f_5^{\gamma,Z}$, which should be the dominant ones [15]. Their contributions to the helicity amplitudes have been given in [14]. As shown there,

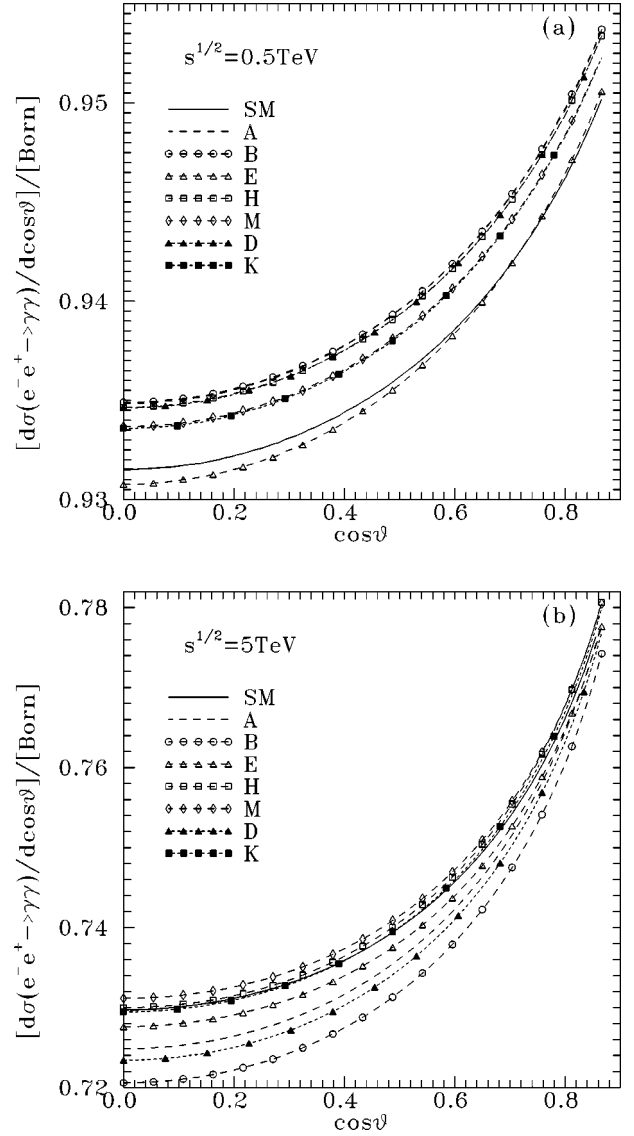


FIG. 2. The ratio of the unpolarized differential cross section $e^-e^+ \rightarrow \gamma\gamma$ to the Born contributions, at 0.5 TeV (a) and 5 TeV (b), for SM and a representative subset of the benchmark MSSM models of [22].

$h_3^{\gamma,Z}$ contributes to the TT and TL $e^+e^- \rightarrow Z\gamma$ amplitudes, and $f_5^{\gamma,Z}$ to the TL $e^+e^- \rightarrow ZZ$ one. There is no contribution to $e^+e^- \rightarrow \gamma\gamma$.

In [15], dynamical models for generating NAGC have been considered. The conclusion of that work was that the contributions to $h_3^{\gamma,Z}$ and $f_5^{\gamma,Z}$ arising from one-loop effects induced by new higher fermions of mass M pertaining to the NP scale, diminish faster than $1/s$, for $s \gg M^2$. So they cannot modify the leading-log SM or MSSM structure, and they are always part of the subleading contributions. But there may exist more general types of NAGC leading to appreciable tree level $h_3^{\gamma,Z}$ and $f_5^{\gamma,Z}$ couplings.

In any case, the processes $e^-e^+ \rightarrow Z\gamma, ZZ$ may be used to constrain such NAGCs, and for this purpose, knowledge of the complete one-loop effects is essential. Such constraints are presented in the next section, assuming LC energies of 0.5 or 5 TeV.

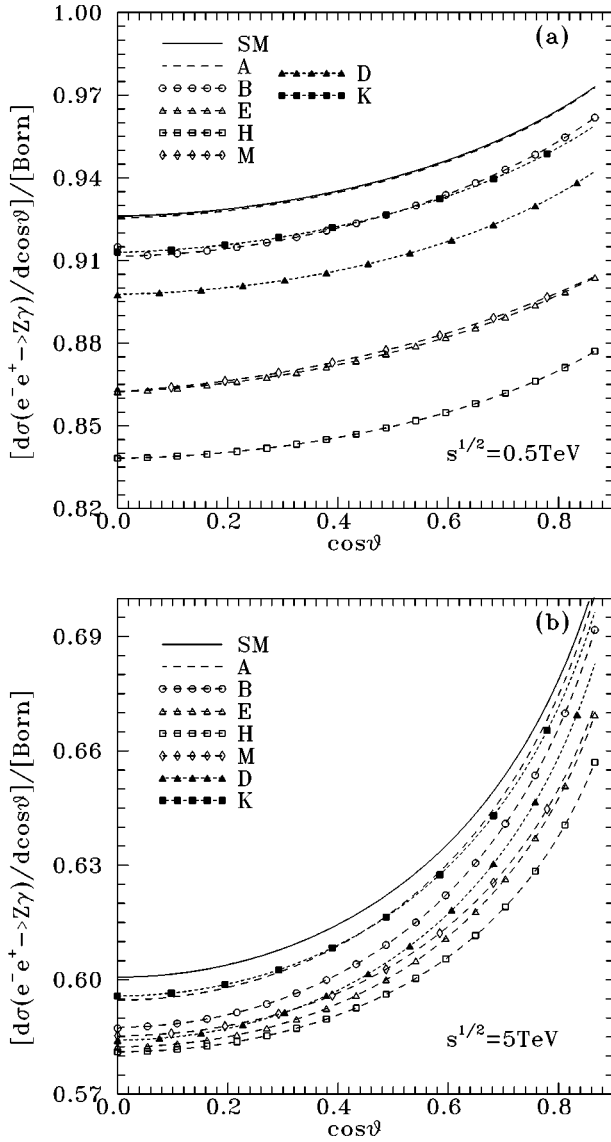


FIG. 3. The ratio of the unpolarized differential cross section $e^-e^+ \rightarrow Z\gamma$ to the Born contribution, at 0.5 TeV (a) and 5 TeV (b), for SM and a representative subset of the benchmark MSSM models of [22].

III. NUMERICAL RESULTS

Here we present the numerical prediction for observables like angular distributions, integrated cross sections, and asymmetries, defined in the Appendix. Most of these observables do not refer to the final gauge boson polarizations. But some remarks concerning the production of specifically transverse or longitudinal Z bosons are also given.

Due to the electron exchange diagrams in the t and u channels, the angular distribution is strongly peaked in the forward and backward directions. Because of detection difficulties along the beam directions, we only consider c.m. scattering angles in the region $30^\circ < \theta < 150^\circ$. The integrated cross sections are thus defined by integrating in this angular region.

The one-loop radiative correction effects to the differential and integrated cross sections are described by the ratios

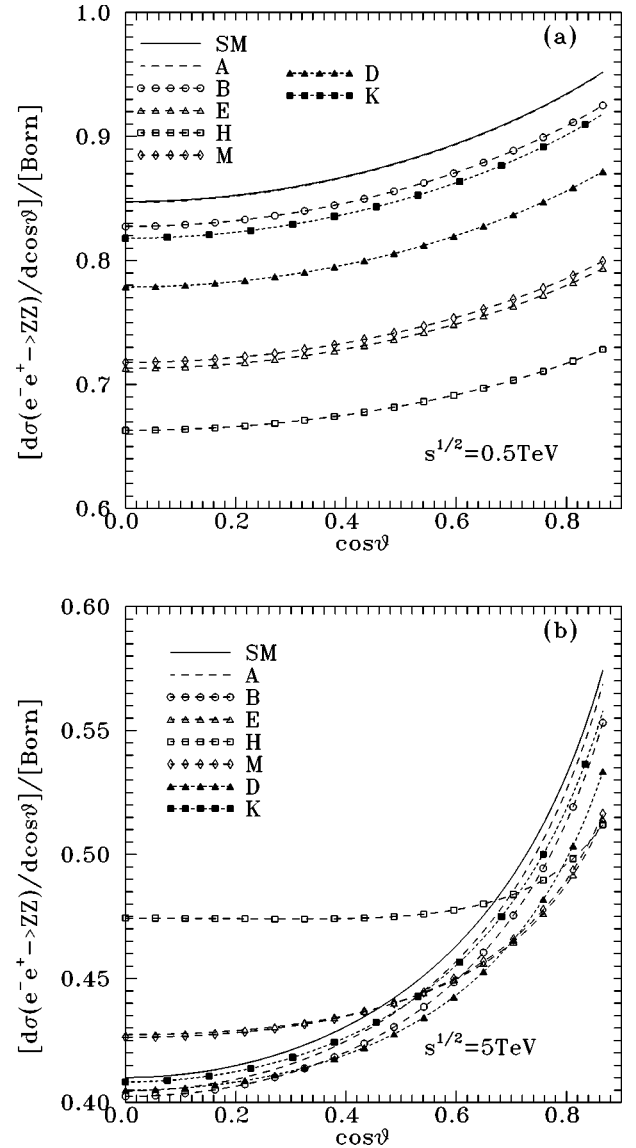


FIG. 4. The ratio of the unpolarized differential cross section $e^-e^+ \rightarrow ZZ$ to the Born contribution, at 0.5 TeV (a) and 5 TeV (b), for SM and a representative subset of the benchmark MSSM models of [22].

to the corresponding Born contributions. Thus the differential cross sections are described in Figs. 2–4 for the SM and a representative set of MSSM SUGRA models suggested in [22], which are consistent with all present particle and cosmological constraints. The effects are always negative and increase with energy and the scattering angle. In the SM at 0.5 TeV, they are about -7% , -8% , and -15% for $\gamma\gamma$, $Z\gamma$, and ZZ production, respectively; while at 5 TeV they correspondingly reach the level of -27% , -40% , and -58% .

The differences between the SM and the various MSSM cases for the differential cross sections, especially at large angles, are within 1.5% for $e^-e^+ \rightarrow \gamma\gamma$, and increase to 10% and 20% for $Z\gamma$ and ZZ production, respectively.

The radiative corrections effects to the integrated unpolarized (summed over all final polarization) cross sections are

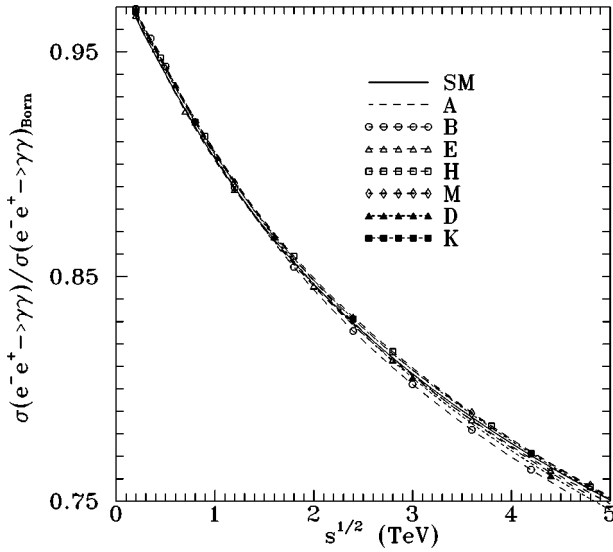


FIG. 5. The ratio of the unpolarized integrated $\sigma(e^-e^+ \rightarrow \gamma\gamma)$ cross section to the Born contribution for SM and a representative subset of the benchmark MSSM models of [22].

described in Figs. 5–7. The above 1 TeV behavior of these cross sections agrees (apart from a model dependent constant term) with the asymptotic leading log expressions (3)–(6), for SM and MSSM, respectively. As pointed out in Sec. II, the main difference between the SM and MSSM predictions at high energy stems from the respective factors $(3 \ln s - \ln^2 s)$ and $(2 \ln s - \ln^2 s)$, which depend only on the overall structure of the theory and are totally independent of any other MSSM parameter. So, an experimental measurement of the coefficient of the linear log term could check the agreement with SM or with MSSM, and even provide hints if any additional NP contribution is needed.

Another interesting quantity is the left-right polarization asymmetry A_{LR} , which is not affected by normalization un-

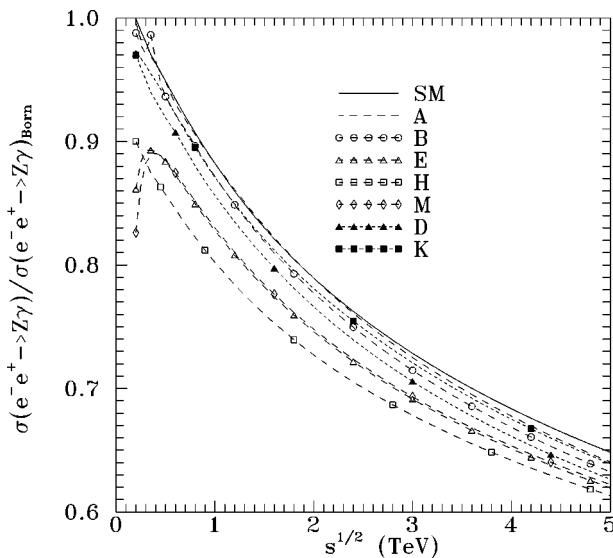


FIG. 6. The ratio of the integrated unpolarized $\sigma(e^-e^+ \rightarrow Z\gamma)$ cross section to the Born contribution, for SM and a set of MSSM models of [22].

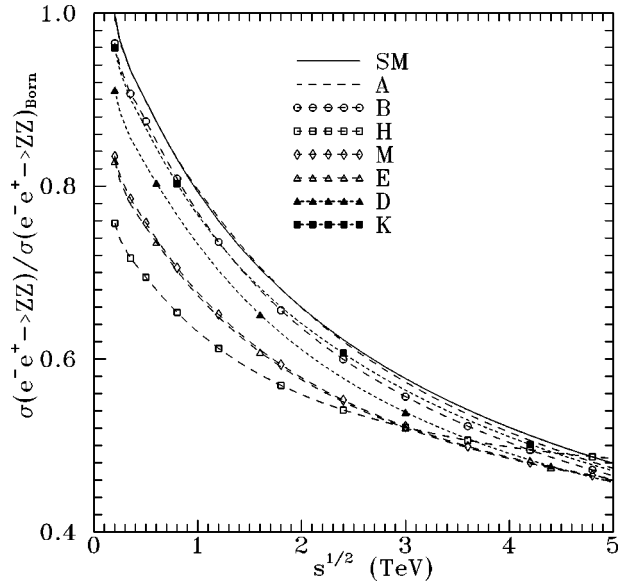


FIG. 7. The ratio of the integrated unpolarized cross section $\sigma(e^-e^+ \rightarrow ZZ)$ to the Born contribution, for SM, and a representative subset of the benchmark MSSM models of [22].

certainties, and its measurement may be extremely interesting experimentally. In this case the Born contribution is constant in energy and satisfies $A_{LR}(\text{Born}) = 0, 0.2181,$ and 0.4164 for $\gamma\gamma, \gamma Z,$ and $ZZ,$ respectively. The radiative corrections can then conveniently be described by the one-loop induced departure from these values. Since the effects are similar to those for the integrated cross sections, we do not present them explicitly.

The above behavior of the unpolarized cross section (or A_{LR} asymmetry) is ensured by the dominance of the TT amplitudes. In $\gamma\gamma$, where only such amplitudes occur, we have checked that by putting an additional constant to the expression for the asymptotic cross section fitted at 5 TeV, we get agreement with the exact one-loop result at the permille level, for energies as low as 0.2 TeV.

In γZ production, the presence of TL amplitudes, which are negligible in the several TeV range,¹ generate corrections below 1 TeV which are at the several percent level and sensitive to the MSSM model considered.

The case of ZZ production is more interesting, because, in addition to the TL and LT components which behave like the ones in γZ , there are also LL components. The Born LL component, which contributes about 10% close to threshold, is strongly depressed at higher energies, behaving like $\sigma_{\text{Born}}^{LL} \sim 1/s^3$. But because of large contributions generated by the Higgs sector,² a logarithmic increase arises above 1 TeV, illustrated in Fig. 8. This happens at a level which is hardly observable, except with very high luminosity colliders. Nevertheless we show it because of its exceptional behavior in the very high energy range. Its dependence on the Higgs

¹The TL cross section behaves like M^2/s^2 at high energies, whereas the TT one behaves like $1/s$, apart from log factors.

²Compare the Goldstone contributions given in Eq. (15).

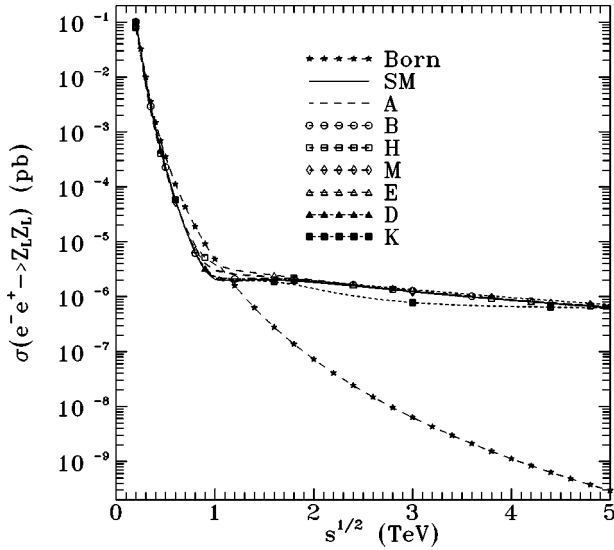


FIG. 8. The integrated cross section for $\sigma(e^-e^+ \rightarrow Z_L Z_L)$, as a function of the energy for SM and a representative subset of the benchmark MSSM models of [22]. For comparison the Born contribution is also given.

mass is rather weak; the relative differences between the cross sections for $m_H=0.3$ TeV or $m_H=1$ TeV, and the one for $m_H=0.113$ TeV being at the permille level.

Constraints on NAGC contributions

We first look at the “normal” NAGC contributions arising from fermionic triangular loops, both in the SM and MSSM. Since these decrease faster than $1/s$ with energy [15], one can only look for NAGC at energies not higher than 1 TeV. In $e^+e^- \rightarrow Z\gamma$ the effects are due to the TT and TL amplitudes; while in $e^+e^- \rightarrow ZZ$ only TL (and LT) amplitudes contribute. However, in the $Z\gamma$ case there is no interference between the NAGC and Born TT amplitudes; since the final gauge boson helicities are equal for the NAGC amplitudes, and opposite for the Born ones. So in both the γZ and ZZ cases, the effects will mainly come from the interference with the weaker Born LT amplitudes, and should be at the permille level around (or below) 1 TeV. We conclude therefore that new NAGC contributions generated by, e.g., triangles involving higher mass fermions, will be marginally observable; unless very high luminosities are available.

We next look at the sensitivity to the “true” NAGC amplitudes, described in a model independent way by the phenomenological coupling constants $h_3^{\gamma,Z}$ for $Z\gamma$, and $f_5^{\gamma,Z}$ for ZZ [14]. Assuming a given experimental accuracy (for example, a conservative 1%) on the unpolarized integrated cross sections σ_{unp} and the left-right asymmetry A_{LR} , we then obtain the NAGC observability limits for such contributions. This is illustrated in Figs. 9(a) and 9(b) for $Z\gamma$ and ZZ production, at energies of 0.5 and 1 TeV.

Note from Figs. 9(a) and 9(b) that the σ_{unp} and A_{LR} constraints are almost orthogonal, allowing a good limitation of both the photon- and Z-NAGCs. This arises because, in $Z\gamma$, σ_{unp} mainly depends on h_3^γ , whereas A_{LR} is more sensitive

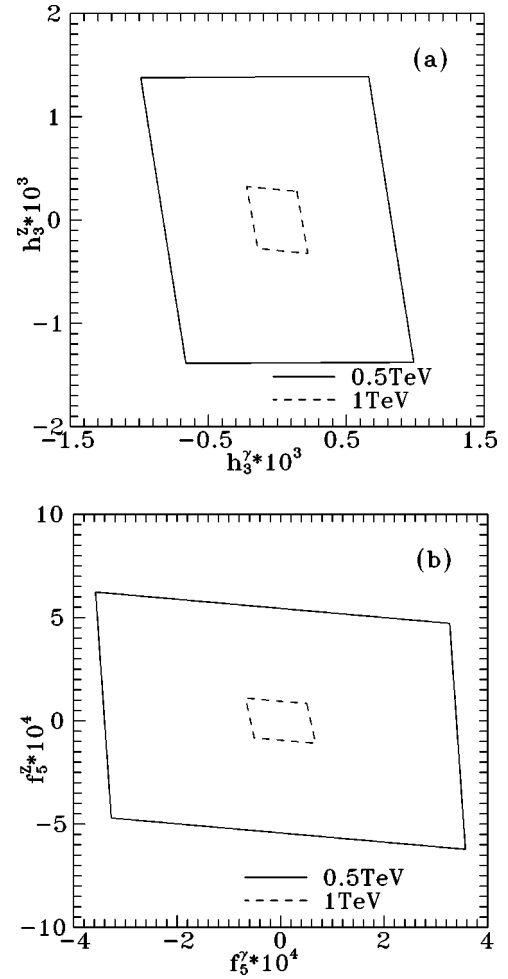


FIG. 9. The NAGC limits from σ_{unp} and A_{LR} measurements assuming an accuracy of 1%, for the processes $e^+e^- \rightarrow Z\gamma$ (a) and $e^+e^- \rightarrow ZZ$ (b).

to h_3^Z . In ZZ the roles of the photon and Z are interchanged, σ_{unp} mainly depending on f_5^Z , and A_{LR} on f_5^γ , due to the different chirality structure of the Born terms. All this can be traced off from the fact that the photon couples vectorially, while the Zee coupling is essentially purely axial.

As seen from Figs. 9(a) and 9(b), the implied sensitivity is likely to increase with energy. We conclude therefore that NP forms inducing the NAGCs $h_3^{\gamma,Z}$, $f_5^{\gamma,Z}$ at the level of 10^{-3} to 10^{-4} , should be observable around 1 TeV.

IV. PHYSICS ISSUES AND CONCLUSIONS

In this paper we have analyzed the behavior of the electroweak corrections to the processes $e^+e^- \rightarrow \gamma\gamma, Z\gamma, ZZ$ at the one loop level, in the context of the SM and the MSSM.

These processes are particularly interesting in various aspects. Their final gauge bosons are easy to detect experimentally, while their theoretical structure provides clean tests of the electroweak interactions. The Born terms are only due to electron exchanges in the t and u channels; contrary to the WW case, there is no s -channel tree level term. Since there are no QCD or Yukawa contributions, the identification of

the electroweak corrections should be very clean.

We have completely computed the one-loop SM and MSSM corrections in order to analyze the contents of the gauge, Higgs, and Goldstone sectors, as well as their supersymmetric counterparts. We have studied how these contributions vary with energy, and how they conspire to generate asymptotically the leading logarithmic terms, and in particular the remarkable difference between the SM combination ($3 \ln s - \ln^2 s$) and the MSSM one ($2 \ln s - \ln^2 s$). This contribution fixes the asymptotic form of the transverse-transverse final gauge boson (TT) amplitudes. At moderate energies, we have also found that the mass-suppressed TL and LL amplitudes play a non-negligible role.

The structures of the angular distributions, integrated cross sections, and left-right asymmetries, for both unpolarized and polarized final states, have also been studied numerically. It was found in particular that the A_{LR} asymmetry shows essentially the same effects as the unpolarized cross section, a feature which may be experimentally interesting in reducing the normalization uncertainties.

In addition to studying the standard and supersymmetric effects, we have considered possible additional NP NAGC contributions, as described by effective Lagrangians. We have shown that the corresponding coupling constants could be constrained at an interesting level.

Summarizing, we can say that the electroweak radiative corrections are large and growing with energy. Starting from a few percent at the energy range of a few hundreds of GeV, they reach 10% already at 1 TeV, and continue growing according to the logarithmic rules. So, in the high energy range they are no longer “small corrections.” They are essential parts of the dynamics, which can be experimentally analyzed at the future colliders, whose accuracy should reach the percent level or even better. For more accurate theoretical predictions, computations of higher orders may be attempted; it has already been claimed that several logarithmic terms exponentiate [12], so that all the features that we have observed at the one-loop level remain true for higher orders also.

We have also shown that measurements of the three processes $e^+e^- \rightarrow \gamma\gamma$, γZ , and ZZ should provide global tests of the basic interactions. A strategy for these tests could be the following. One could first try to compare the high energy behavior of the cross sections and left-right asymmetries with the SM predictions [containing in particular the ($3 \ln s - \ln^2 s$) term]. If there is no new particle produced, SM may seem to be a reasonable assumption, and one would either check its consistency or, if the check fails,³ we would be led to anticipate some form of NP.

Another situation may be that many candidates for supersymmetric particles are found, with masses considerably smaller than the highest collider energy attainable. One should then compare the high energy behavior with the MSSM prediction [containing in particular the ($2 \ln s - \ln^2 s$) term] and again we could check whether a global agreement appears. If there are still some departures indicating the need

for additional NP effects, a comparison of the three processes $\gamma\gamma$, $Z\gamma$, ZZ may provide a hint for their origin; particularly if NP is related to NAGC couplings or to some other anomalous properties of the Z boson. We also note that a measurement of the coefficient of the double log term could check if there are no higher gauge bosons acting.

In conclusion, the three processes studied here present a large panel of interesting properties. They are extremely simple at the Born level, but extremely rich in the supplied information at the radiative corrections level. The $\gamma\gamma$, $Z\gamma$, and ZZ final states are complementary for the study of the gauge (gaugino) sector in the MSSM models, the Higgs sector, and the search for neutral anomalous gauge couplings.

We have thus seen one more aspect of the fact that in the several TeV domain the electroweak interactions start becoming strong. The processes studied here illustrate this property and should be considered as part of the research program at the future high energy colliders, demanding for the highest luminosities. In some respect, the tests supplied by ($e^-e^+ \rightarrow \gamma\gamma$, $Z\gamma$, ZZ), are in the same spirit as the high precision tests performed with $g-2$ measurements, or with Z peak physics. They should provide global checks of the validity of the SM or MSSM theory.

ACKNOWLEDGMENT

This work was supported by “Programme d’Actions Intégrées Franco-Hellenique, Platon 04100 UM.”

APPENDIX: KINEMATICAL DETAILS

The considered process is

$$e^-(\lambda, l) + e^+(\lambda', l') \rightarrow V(e, p) + V'(e', p'), \quad (\text{A1})$$

where (l, l') are the incoming electron and positron momenta, and (λ, λ') their helicities. The outgoing neutral gauge bosons Z or γ are generally denoted as V and V' , their momenta as (p, p') , respectively, the complex conjugate of their polarization vectors as (e, e') , and their corresponding helicities as (μ, μ') . We also define

$$q = l - p = p' - l', \quad q' = l - p' = p - l', \\ s = (l + l')^2 = (p + p')^2, \quad t = q^2, \quad u = q'^2.$$

The c.m. scattering angle between \vec{l} and \vec{p} is denoted by θ .

The electron mass is throughout neglected, implying $\lambda' = -\lambda = \pm 1/2$. Consequently there are at most 18 helicity amplitudes written as

$$F_{\lambda, \mu, \mu'} \equiv F[e^-(\lambda, l)e^+(\lambda' = -\lambda, l') \\ \rightarrow V(e(\mu), p) V'(e'(\mu'), p')] \\ = \sum_{j=1,9} \bar{v}(\lambda', l') I_j N_j(s, t, u, \lambda) u(\lambda, l), \quad (\text{A2})$$

in terms of nine Lorentz invariant forms I_j ($j=1,9$) defined below.

³I.e., a disagreement with the predicted high energy behavior is identified.

$$\begin{aligned}
 I_1 &= (e \cdot l)(\gamma \cdot e'), & I_2 &= (e' \cdot l)(\gamma \cdot e), \\
 I_3 &= (e \cdot l)(e' \cdot l)(\gamma \cdot p), \\
 I_4 &= (e \cdot e')(\gamma \cdot p), & I_5 &= (e \cdot p')(\gamma \cdot e'), \\
 I_6 &= (e \cdot p')(e' \cdot l)(\gamma \cdot p), & & \\
 I_7 &= (e' \cdot p)(\gamma \cdot e), & I_8 &= (e' \cdot p)(e \cdot l)(\gamma \cdot p), \\
 I_9 &= (e \cdot p')(e' \cdot p)(\gamma \cdot p).
 \end{aligned} \tag{A3}$$

Their coefficients, split according to the electron-helicity, define the invariant amplitudes as

$$N_j(s, t, u, \lambda) \equiv N_j^L(s, t, u)P_L + N_j^R(s, t, u)P_R, \tag{A4}$$

where

$$P_L = \frac{1}{2} - \lambda, \quad P_R = \frac{1}{2} + \lambda. \tag{A5}$$

In the specific case of the process $e^-e^+ \rightarrow \gamma\gamma$, only four transverse-transverse amplitudes appear, which are described through the invariant functions N_1, N_2, N_3, N_4 .

In the case of $e^-e^+ \rightarrow Z\gamma$, where the gauge boson polarization and momenta are defined by $Z(e, p)$ and $\gamma(e', p')$, the process is most generally described by the six invariant amplitudes N_1, \dots, N_6 .

Finally, for $e^-e^+ \rightarrow ZZ$, the complete set of the N_1, \dots, N_9 amplitudes is needed for a complete description.

1. Observables

The polarized differential cross section is written as

$$\frac{d\sigma(\lambda, \mu, \mu')}{d \cos \theta} = \frac{\beta}{32\pi s} C_{stat} |F_{\lambda, \mu, \mu'}|^2, \tag{A6}$$

where $C_{stat} = 1/2, 1/2,$ and 1 for $\gamma\gamma, ZZ,$ and γZ , respectively. The integrated cross sections for definite polarizations are

$$\sigma(\lambda, \mu, \mu') = \int_{-c}^c d \cos \theta \frac{d\sigma(\lambda, \mu, \mu')}{d \cos \theta}, \tag{A7}$$

where $c \equiv \cos \theta_{min}$ is an angular cut (fixed at $\theta_{min} = 30^\circ$ in the numerical applications).

For longitudinally polarized e^\pm beams, the left-right polarization asymmetry is defined as

$$A_{LR}(\mu, \mu') = \frac{\sigma\left(-\frac{1}{2}, \mu, \mu'\right) - \sigma\left(+\frac{1}{2}, \mu, \mu'\right)}{\sigma\left(-\frac{1}{2}, \mu, \mu'\right) + \sigma\left(+\frac{1}{2}, \mu, \mu'\right)}. \tag{A8}$$

2. The Born terms

These are due to electron exchange in the t and u channels. In terms of the invariant amplitudes defined in Eq. (A4), they are written as

$$N_j^{\text{Born}} = N_j^{\text{Born}, t} + N_j^{\text{Born}, u}, \tag{A9}$$

and for all processes it is found that

$$N_{3,9}^{\text{Born}, t} = N_{3,9}^{\text{Born}, u} = 0. \tag{A10}$$

The rest of the invariant amplitudes are:

$e^-e^+ \rightarrow \gamma\gamma$.

$$N_1^{\text{Born}, t} = N_2^{\text{Born}, t} = N_4^{\text{Born}, t} = -\frac{e^2}{t} P_L - \frac{e^2}{t} P_R,$$

$$N_1^{\text{Born}, u} = N_2^{\text{Born}, u} = -N_4^{\text{Born}, u} = -\frac{e^2}{u} P_L - \frac{e^2}{u} P_R. \tag{A11}$$

$e^-e^+ \rightarrow ZZ$.

$$N_1^{\text{Born}, t} = N_2^{\text{Born}, t} = N_4^{\text{Born}, t} = -\frac{s}{t - m_Z^2} N_5^{\text{Born}, t} = -\frac{s}{2} N_6^{\text{Born}, t}$$

$$= -\frac{s}{s - t + m_Z^2} N_7^{\text{Born}, t} = \frac{s}{2} N_8^{\text{Born}, t} = -\frac{g_{ZL}^2}{t} - \frac{g_{ZR}^2}{t},$$

$$N_1^{\text{Born}, u} = N_2^{\text{Born}, u} = -N_4^{\text{Born}, u} = \frac{-s}{s - u + m_Z^2} N_5^{\text{Born}, u}$$

$$= \frac{-s}{2} N_6^{\text{Born}, u} = \frac{-s}{u - m_Z^2} N_7^{\text{Born}, u} = \frac{s}{2} N_8^{\text{Born}, u}$$

$$= -\frac{g_{ZL}^2}{u} - \frac{g_{ZR}^2}{u}, \tag{A12}$$

with

$$g_{ZL} = e \frac{(2s_W^2 - 1)}{2s_W c_W}, \quad g_{ZR} = e \frac{s_W}{c_W}. \tag{A13}$$

$e^-e^+ \rightarrow Z\gamma$.

$$\frac{s}{s - m_Z^2} N_1^{\text{Born}, t} = \frac{s}{s + m_Z^2} N_2^{\text{Born}, t} = N_4^{\text{Born}, t} = -\frac{s}{t - m_Z^2} N_5^{\text{Born}, t}$$

$$= -\frac{s}{2} N_6^{\text{Born}, t} = \frac{e g_{ZL}}{t} P_L + \frac{e g_{ZR}}{t} P_R,$$

$$\left(\frac{s}{s - m_Z^2}\right) N_1^{\text{Born}, u} = \left(\frac{s}{s + m_Z^2}\right) N_2^{\text{Born}, u} = -N_4^{\text{Born}, u}$$

$$= \left(\frac{-s}{s - u}\right) N_5^{\text{Born}, u} = \frac{-s}{2} N_6^{\text{Born}, u}$$

$$= \frac{e g_{ZL}}{u} P_L + \frac{e g_{ZR}}{u} P_R. \tag{A14}$$

- [1] “Opportunities and Requirements for Experimentation at a Very High Energy e^+e^- Collider,” SLAC-329 (1928); Proceedings of the Workshops on Japan Linear Collider, KEK Reports 90-2, 91-10, and 92-16; P.M. Zerwas, DESY 93-112, 1993; Proceedings of the Workshop on e^+e^- Collisions at 500 GeV: The Physics Potential, DESY 92-123A,B(1992), C(1993), D(1994), E(1997), edited by P. Zerwas; E. Accomando *et al.*, Phys. Rep. C **299**, 1 (1998).
- [2] “The CLIC study of a multi-TeV e^+e^- linear collider,” CERN-PS-99-005-LP (1999).
- [3] I.F. Ginzburg, G.L. Kotkin, V.G. Serbo, and V.I. Telnov, Nucl. Instrum. Methods Phys. Res. **205**, 47 (1983); I.F. Ginzburg, G.L. Kotkin, V.G. Serbo, S.L. Panfil, and V.I. Telnov, *ibid.* **219**, 5 (1984); J.H. Kühn, E. Mirkes, and J. Steegborn, Z. Phys. C **57**, 615 (1993); V. Telnov, Int. J. Mod. Phys. A **15**, 2577 (2000); Nucl. Instrum. Methods Phys. Res. A **455**, 63 (2000); Int. J. Mod. Phys. A **13**, 2399 (1998); hep-ex/9805002; Nucl. Phys. B (Proc. Suppl.) **82**, 359 (2000); I.F. Ginzburg, *ibid.* **82**, 367 (2000); R. Brinkman, Nucl. Instrum. Methods Phys. Res. A **406**, 13 (1998); D.S. Gorbunov, V.A. Il'yn, and V. Telnov, in *Proceedings of the International Workshop on High Energy Photon Colliders*, 2000, DESY Hamburg, Germany [Nucl. Instrum. Methods A **472**, 171 (2001)].
- [4] V.V. Sudakov, Sov. Phys. JETP **3**, 65 (1956); *Landau-Lifshits: Relativistic Quantum Field Theory IV Tome* (MIR, Moscow, 1972).
- [5] M. Kuroda, G. Moulataka, and D. Schildknecht, Nucl. Phys. **B350**, 25 (1991); G. Degrassi and A. Sirlin, Phys. Rev. D **46**, 3104 (1992); W. Beenakker *et al.*, Nucl. Phys. **B410**, 245 (1993); Phys. Lett. B **317**, 622 (1993); A. Denner, S. Dittmaier, and R. Schuster, Nucl. Phys. **B452**, 80 (1995); A. Denner, S. Dittmaier, and T. Hahn, Phys. Rev. D **56**, 117 (1997); P. Ciafaloni and D. Comelli, Phys. Lett. B **446**, 278 (1999); A. Denner and S. Pozzorini, Eur. Phys. J. C **18**, 461 (2001); **21**, 63 (2001).
- [6] M. Beccaria, P. Ciafaloni, D. Comelli, F. Renard, and C. Verzegnassi, Phys. Rev. D **61**, 073005 (2000); **61**, 011301(R) (2000).
- [7] M. Beccaria, F.M. Renard, and C. Verzegnassi, Phys. Rev. D **64**, 073008 (2001).
- [8] M. Beccaria, F.M. Renard, and C. Verzegnassi, hep-ph/0203254.
- [9] M. Beccaria, F.M. Renard, and C. Verzegnassi, Phys. Rev. D **63**, 095010 (2001); **63**, 053013 (2001).
- [10] J. Layssac and F.M. Renard, Phys. Rev. D **64**, 053018 (2001).
- [11] M. Beccaria, M. Melles, F.M. Renard, and C. Verzegnassi, Phys. Rev. D **65**, 093007 (2002).
- [12] M. Ciafaloni, P. Ciafaloni, and D. Comelli, Nucl. Phys. **B589**, 4810 (2000); V.S. Fadin, L.N. Lipatov, A.D. Martin, and M. Melles, Phys. Rev. D **61**, 094002 (2000); J.H. Kühn, A.A. Penin, and V.A. Smirnov, Eur. Phys. J. C **17**, 97 (2000); M. Melles, hep-ph/0104232; J.H. Kühn, S. Moch, A.A. Penin, and V.A. Smirnov, Nucl. Phys. **B616**, 286 (2001); M. Melles, Eur. Phys. J. C **24**, 193 (2002); M. Melles, Phys. Rev. D **63**, 034003 (2001); **64**, 014011 (2001); **64**, 054003 (2001); Phys. Lett. B **495**, 81 (2000); W. Beenakker and A. Werthenbach, Phys. Lett. B **489**, 148 (2000); Nucl. Phys. **B630**, 3 (2002); M. Hori, H. Kawamura, and J. Kodaira, Phys. Lett. B **491**, 275 (2000).
- [13] M. Bohm and T. Sack, Z. Phys. C **33**, 157 (1986); **35**, 119 (1987); A. Denner and T. Sack, Nucl. Phys. **B306**, 221 (1988).
- [14] K. Hagiwara, R.D. Peccei, and D. Zeppenfeld, Nucl. Phys. **B282**, 253 (1987); G.J. Gounaris, J. Layssac, and F.M. Renard, Phys. Rev. D **61**, 073013 (2000).
- [15] G.J. Gounaris, J. Layssac, and F.M. Renard, Phys. Rev. D **62**, 073013 (2000); **62**, 073012 (2000).
- [16] D. Choudhury, S. Dutta, S. Rakshit, and S. Rindani, Int. J. Mod. Phys. A **16**, 4891 (2001).
- [17] ALEPH, DELPHI, L3, OPAL, LEP Electroweak Working Group and SLD Heavy Flavor and Electroweak Groups, D. Abbaneo *et al.*, hep-ex/0112021; P. Bambade *et al.*, “Study of Trilinear Gauge Boson Couplings ZZZ , $ZZ\gamma$ and $Z\gamma\gamma$,” DELPHI 2001-097 CONF 525, contributed to EPS HEP 2001 Conference in Budapest; L3, M. Acciarri *et al.*, Phys. Lett. B **497**, 23 (2001); J. Alcaraz, Phys. Rev. D **65**, 075020 (2002).
- [18] See, e.g., W. Hollik, in *Precision Tests of the Standard Electroweak Model*, edited by P. Langacker (World Scientific, Singapore, 1993), p. 37; MPI-Ph-93-021, BI-TP-93-16.
- [19] G.J. Gounaris, J. Layssac, and F.M. Renard, hep-ph/0207273.
- [20] J. Rosiek, Phys. Rev. D **41**, 3464 (1990); hep-ph/9511250 (E).
- [21] M.M. El Kheishen, A.A. Shafik, and A.A. Aboshousha, Phys. Rev. D **45**, 4345 (1992); V. Barger, M.S. Berger, and P. Ohman, *ibid.* **49**, 4908 (1994); G.J. Gounaris, C. Le Mouél, and P.I. Porfyriadis, *ibid.* **65**, 035002 (2002); G.J. Gounaris and C. Le Mouél, *ibid.* **66**, 055007 (2002).
- [22] M. Battaglia, A. De Roeck, J. Ellis, F. Giannotti, K.T. Matchev, K.A. Olive, L. Pape, and G. Wilson, Eur. Phys. J. C **22**, 535 (2001); S. P. Martin, <http://zippy.physics.niu.edu/modellines.html>; S. P. Martin, S. Moretti, J. Qian, and G. W. Wilson, Snowmass P3-46.
- [23] B.C. Allanach *et al.*, Eur. Phys. J. C **25**, 113 (2002).